

Optimization-based reference calculation for Modular Multilevel Converters in balanced and unbalanced network conditions

Daniel Westerman Spier¹, Eduardo Prieto-Araujo², Joaquim López-Mestre¹, and Oriol Gomis-Bellmunt²

¹Control Intel·ligent de l'Energia, coop (CINERGIA).

Carrer Can Baletes, 7, 08310 Argentona, Spain

Email: daniel.westerman@cinergia.coop and quimlopez@cinergia.coop

²CITCEA-UPC, Polytechnic University of Catalonia.

Avinguda Diagonal, 647, 08028 Barcelona, Spain

Email eduardo.prieto-araujo@upc.edu and oriol.gomis@upc.edu

Acknowledgment

This project has received funding from the European Union's Horizon 2020 research and innovation programme under the Marie Skłodowska-Curie grant agreement no. 765585. This document reflects only the author's views; the European Commission is not responsible for any use that may be made of the information it contains. This work has also been partially funded by FEDER/Ministerio de Ciencia, Innovación y Universidades - Agencia Estatal de Investigación, Project RTI2018-095429-B-I00 and by the ICREA Academia program.

Abstract

The paper addresses an optimization-based algorithm to calculate the references of the Modular Multilevel Converter (MMC) during normal and constrained scenarios (when the prioritization of quantities is required). The optimization problem prioritizes to satisfy the positive- and negative-sequence active and reactive current set-points demanded by the Transmission System Operator (TSO) through the corresponding grid code. If the TSO's requirements are achieved, the algorithm minimizes the arm impedances losses. Otherwise, it attempts to reduce the error between the current components and the TSO's current set-points. The optimization-based current reference calculation is derived based on the steady-state equations of the MMC, considering the maximum currents that can flow through the MMC's arms, the maximum and minimum arm applied voltages and the maximum sub-module capacitor's voltage. Simulation in the time-domain have been conducted and the results indicate that this method can be potentially employed to calculate the converter's references during both normal and faulted conditions.

Keywords

«Modular Multilevel Converters (MMC)», «HVDC», «Optimization algorithm».

Introduction

The modular multilevel converter (MMC) has become the selected choice for High Voltage Direct Current (HVDC) systems, due to its lower switching frequencies, higher output voltage quality and easier adaptation to higher voltages compared to two- and three-level Voltage Source Converters (VSC) [1]. The MMC has additional degrees of freedom that must properly be exploited in order to not only improve the converter's performance during AC network voltage sags [2], but also to meet with the grid code requirements (in terms of active and reactive current components to be injected into the AC grid during such faults). Relevant previous works have been done regarding the steady-state analysis of the converter's quantities during normal and faulted scenarios [3–6], but limited references can be found

when the grid operator constraints (for active and reactive current injection during AC grid faults) are considered throughout the steady-state modelling.

In this paper, a multi-objective optimization-based steady-state model of the MMC is introduced to calculate the converter's current references. Such optimization algorithm can be employed under different AC and DC network voltage conditions, where both the grid code restraints and the MMC's design limits are considered and respected. To validate the suggested method, different case studies are presented comparing the outputs obtained from the steady-state model with the time-domain simulations of the converter.

MMC system description

The schematic model of the three-phase MMC is shown in Fig. 1. The converter has three phase-legs, in which each one consists of two stacks of N_{arm} sub-modules (SMs), also known as upper and lower arms. Due to its simplicity and lower costs, the half-bridge topology is widely employed as the SMs structure in MMC-HVDC applications [7]. For steady-state modelling purposes, the phasor notation $\underline{X}^k = X_r^k + jX_i^k = X^k \angle \theta^k$ will be adopted, with $x(t) = X^k \text{Re}\{e^{j(\omega t + \theta^k)}\} \forall k \in (a, b, c)$. The main quantities of interest for each phase can be summarized as: the AC grid voltages \underline{U}_g^k ; the upper and lower arms applied voltages $\underline{U}_{u,l}^k$; the upper and lower DC grid voltages $U_{u,l}^{DC}$; the voltage between the 0 DC reference node and the neutral n of the AC three-phase system \underline{U}_{0n} ; the upper and lower arm currents $I_{u,l}^k$; the AC grid current I_s^k ; the arm impedances R_a and L_a ; the grid equivalent resistance and inductance R_s and L_s ; and the sub-module capacitors C_{SM} .

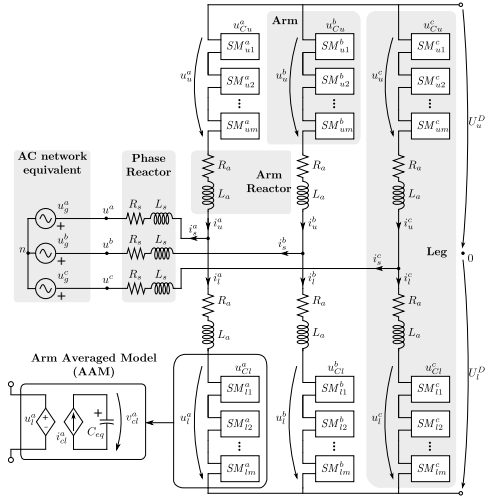


Fig. 1: Complete model of the MMC converter.

Description of the optimization problem

In this section, an optimization algorithm is introduced to calculate the MMC's quantities during balanced and unbalanced AC network scenarios ensuring that its internal quantities are kept within its limits. The optimal model is based on the converter analysis derived in [8], which considers that both the AC and DC networks can be either in balanced or unbalanced voltage conditions. The model also assumes that the values for the AC grid voltages U_g^k and the positive- and negative- sequence components of the active $I_p^{+,-}$ and reactive $I_q^{+,-}$ currents to be injected by the MMC are known parameters. Whereby the former current magnitudes are imposed based on the Transmission System Operator (TSO) requirements and are calculated assuming the positive- and negative-sequence voltage components of the AC grid $U_g^{+,-}$. The general optimization problem can be mathematically described as

$$\begin{aligned}
& \underset{\substack{I_{u,l}^k, I_{u,l}^{kDC}, U_{u,l}^k, U_{u,l}^{kDC}, \\ U_{n0}, \alpha^{+,-}, \beta^{+,-}}}{\text{minimize}} & \lambda_{losses} \left(R_a \sum_{k=a}^c \left(I_u^k{}^2 + I_l^k{}^2 + I_u^{kDC}{}^2 + I_l^{kDC}{}^2 \right) \right) - \lambda_{I_p^+} \alpha^+ - \lambda_{I_q^+} \beta^+ + \lambda_{I_p^-} \alpha^- + \lambda_{I_q^-} \beta^- \\
& \text{subject to} & \text{Equality constraints,} \\
& & I_s^k \leq I_{max}^{AC}, \\
& & I_{u,l}^k + I_{u,l}^{kDC} \leq I_{max}^{arm}, \\
& & U_{Cu,l,max}^k \leq U_{C,max}, \\
& & 0 \leq U_{u,l}^k + U_{u,l}^{kDC} \leq U_{Cu,l,min}^k, \\
& & 0 \leq \alpha^{+,-} \leq 1, \\
& & 0 \leq \beta^{+,-} \leq 1
\end{aligned} \tag{1}$$

where, the objective function, given in (1), consists of the term regarding the arm impedance losses plus four coefficients, $\alpha^{+,-}$ and $\beta^{+,-}$, which are employed to regulate the levels of positive- and negative-sequence active and reactive current components to be injected/absorbed by the AC grid, respectively, in order to comply with the grid operator requirements. These coefficients and term are prioritized according to the values used in the optimal weights $\lambda_{I_p^{+,-}}, \lambda_{I_q^{+,-}}$ and λ_{losses} . This paper adopts $\lambda_{I_q^+} \gg \lambda_{I_q^-} \gg \lambda_{I_p^+} \gg \lambda_{I_p^-} \gg \lambda_l$; thus, the highest priority is given to the reactive currents followed by the active currents (the positive-sequence has higher priority for same current component), and by the inductance losses. The terms in (1) which have positive signs are minimized by the optimization, whereas the negative ones are maximized. Therefore, the algorithm attempts to minimize both losses and negative-sequence current components and to maximize the positive-sequence current components. Following, the linear and nonlinear optimization constraints are presented in the form of equalities and inequalities constraints that are used to ensure the fulfilment of the converter's technical restrictions.

Equality constraints

In this section the equality constraints which the objective function in (1) is subjected to are derived. However, such constraints must consider not only the Transmission System Operator's (TSO) active I_p and reactive I_q current set-points demands but also the converter's limits. Next, the procedures to mathematically describe the MMC voltages and currents (calculated based on the grid-code requirements and physical limitations of the converter) are given, and are part of the optimization problem (see (1)). In order to obtain such equations, the superposition principle is employed allowing the AC and DC quantities to be decoupled into two different circuits (see Fig. 2) and analyzed separately.

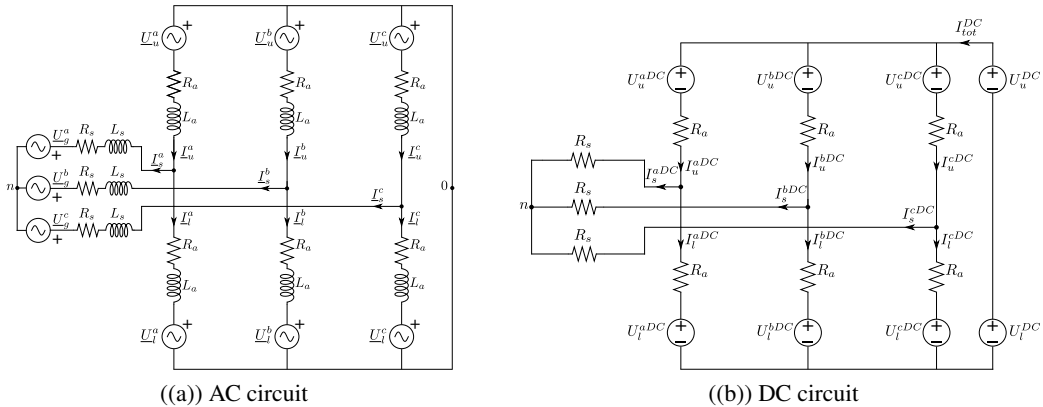


Fig. 2: AC and DC circuit models of the MMC.

AC equality constraints based on circuit analysis

The AC model of the MMC is shown in Fig. 2a, which is obtained by short-circuiting the DC network and assuming that the arms' voltages have purely AC components. By applying Kirchhoff Current and Voltage Laws (KCL and KVL) in the circuit, the AC current and voltage relations can be obtained as

$$I_s^k = I_u^k - I_l^k \tag{2}$$

$$\underline{U}_{0n} = \underline{U}_g^k + \underline{Z}_s(I_u^k - I_l^k) + \underline{Z}_a I_u^k + \underline{U}_u^k \quad (3)$$

$$\underline{U}_{0n} = \underline{U}_g^k + \underline{Z}_s(I_u^k - I_l^k) - \underline{Z}_a I_l^k - \underline{U}_l^k \quad (4)$$

where, \underline{U}_{0n} is the voltage drop across the 0 DC reference node and the neutral n of the AC three-phase system and, \underline{Z}_s and \underline{Z}_a are the phase reactor and MMC's arm impedances, respectively. The final equation of the AC model prevents the undesired circulation of AC currents through the DC network. This can be mathematically imposed by assuming that the sum of the upper arm's currents is equal to zero, shown as follows

$$I_u^a + I_u^b + I_u^c = 0 \quad (5)$$

DC equality constraints based on circuit analysis

The DC analysis of the MMC is derived similarly to the one performed for the AC model. Short-circuiting the AC voltage sources, the DC scheme of the converter can be obtained as it is shown in Fig. 2b. Applying KVL and KCL to the DC circuit, the following relations can be obtained

$$U_u^{DC} + U_l^{DC} = U_u^{kDC} + U_l^{kDC} + R_a (I_u^{kDC} + I_l^{kDC}) \quad (6)$$

$$2(-U_u^{aDC} + U_l^{aDC}) + (U_u^{bDC} - U_l^{bDC} + U_u^{cDC} - U_l^{cDC}) = (U_u^{bDC} - U_l^{bDC} - U_u^{cDC} + U_l^{cDC}) = 0 \quad (7)$$

$$I_u^{kDC} - I_l^{kDC} = 0 \quad (8)$$

$$I_{tot}^{DC} = I_u^{aDC} + I_u^{bDC} + I_u^{cDC} \quad (9)$$

where (6) describes the DC voltages in the converter, (7) is employed to ensure that no DC voltages are reflected into the AC side of the converter. In addition, (8) indicates that no DC currents flow into the AC grid and (9) express the total DC current of the system.

AC equality constraints based on TSO's requirements

The magnitude of the AC grid current I_s^k (which used in the optimization problem) can be related to the active and reactive current set-points demanded by the TSO, as shown in (10). Furthermore, the grid operator may require additional injection of active or reactive currents, according to the magnitude of the positive- and negative-sequence components of the AC grid voltages $U_g^{+,-}$ during a voltage sag event, in order to provide frequency [9] or voltage [10] supports. However, the final magnitude of I_s^k to comply with the grid code demands may exceed the converter's design limits. Therefore, the parameters ($\alpha^{+,-}$ and $\beta^{+,-}$) are used not only to adapt the amount of active and reactive currents to be injected (in case of the AC grid current magnitude to reach its limit) but also to allow the prioritization among such current components. Under normal conditions, all the coefficients should be equal to 1, but for other operating conditions, $\alpha^{+,-}$ and $\beta^{+,-}$ must be adjusted by the objective function (see (1)) in order to comply with the mentioned constraints.

$$\begin{bmatrix} I_{s_r}^{+,-} \\ I_{s_i}^{+,-} \end{bmatrix} = \begin{bmatrix} \cos(\theta^{+,-}) & -\sin(\theta^{+,-}) \\ \sin(\theta^{+,-}) & \cos(\theta^{+,-}) \end{bmatrix} \cdot \begin{bmatrix} \alpha^{+,-} \cdot I_p^{+,-} \\ \beta^{+,-} \cdot I_q^{+,-} \end{bmatrix} \rightarrow \begin{bmatrix} I_s^a \\ I_s^b \\ I_s^c \end{bmatrix} = \begin{bmatrix} 1 & 1 & 1 \\ p^2 & p & 1 \\ p & p^2 & 1 \end{bmatrix} \cdot \begin{bmatrix} I_{s_r}^+ + j \cdot I_{s_i}^+ \\ I_{s_r}^- + j \cdot I_{s_i}^- \end{bmatrix} \quad (10a)$$

where θ^+ and θ^- are the AC network phase-angles for the positive- and negative-sequence components, respectively, and $p = e^{j\frac{2\pi}{3}}$.

Non-linear equality constraint

The final equality constraint required by optimization problem defines the power balance within the storage units of the MMC. To hold steady-state conditions, the AC and DC active power exchanged within the halves of the converter should be equal; thus the stored energy in each arm of MMC are balanced (neither charging or discharging the equivalent arm capacitors). This condition can be mathematically described as follows

$$P_{u,l}^{kAC} = P_{u,l}^{kDC} \rightarrow U_{u,l_r}^k I_{u,l_r}^k + U_{u,l_i}^k I_{u,l_i}^k = U_{u,l}^{kDC} I_{u,l}^{kDC} \quad (11)$$

Inequalities

The voltage and current limitations of the converter are established by different inequality constraints which are expressed as

$$I_{s_{ref}}^k \leq I_{max}^{AC}, \quad I_{u,l}^k + I_{u,l}^{kDC} \leq I_{max}^{arm} \quad (12a)$$

$$U_{Cu,lmax}^k \leq U_{Cmax} \quad (12b)$$

$$0 \leq U_{u,l}^{kDC} + \sqrt{2}U_{u,l}^k \leq U_{Cu,lmin}^k \quad (12c)$$

$$0 \leq \alpha^+ \leq 1, \quad 0 \leq \beta^+ \leq 1, \quad 0 \leq \alpha^- \leq 1, \quad 0 \leq \beta^- \leq 1 \quad (12d)$$

where I_{max}^{AC} and I_{max}^{arm} are the maximum allowed currents that can circulate through the AC grid and the MMC's arms, respectively, whereas U_{Cmax} is the peak voltage level accepted into the equivalent arms' capacitors voltage. The terms $U_{Cu,lmax}^k$ and $U_{Cu,lmin}^k$ in (12b) and (12c) are calculated based on [8], and they are used to ensure that the equivalent arm capacitors do not exceed their maximum voltage levels and to avoid over-modulations. Finally, (12d) limits the optimal coefficients.

Case Study

In this section, the results of the suggested optimal reference calculation method are shown for balanced and unbalanced AC grid voltage sag conditions. The optimization results are obtained with Matlab[®] using *fmincon* which are later applied to an average model of the MMC in Matlab Simulink[®]. The time-domain responses of the converter and the optimization outputs are compared in order to verify the applicability of the proposed algorithm. The system parameters for the case studies are similar to the ones used in [8] and the optimal weights are $\lambda_{I_q^+} = 10^6$, $\lambda_{I_q^-} = 10^3$, $\lambda_{I_p^+} = 1$, $\lambda_{I_p^-} = 10^{-3}$ and $\lambda_I = 10^{-9}$.

In Fig. 3, time-domain simulations of the MMC for balanced and unbalanced voltage sags are shown. It can be noted that all quantities obtained by the optimization algorithm are in close agreement with the ones from the averaged model of the converter and kept within their design limits. In Fig. 3a, it is considered that the AC network is operated under balanced conditions, but the MMC's upper DC pole suffers a voltage drop equals to 15% (from 320 kV to 272kV). In Fig. 3b, a three-phase balanced fault is displayed and it can be observed that the reactive power of the AC grid presents a negative value (indicating the injection of reactive current), whereas the active power is equal to zero (since full reactive support is provided and such component is prioritized during the fault). For Figs. 3c and 3d, different unbalanced AC voltage sags are depicted whereby the converter is also providing full support to the grid. However, due to the unbalanced characteristics of the fault, the reactive current injected into the grid contains both positive- and negative-sequence components. Based on the magnitude of $U_g^{+,-}$ and the priorities selected in (1), full voltage support is provided by I_q^+ , while partial support is given through the negative-sequence I_q^- .

Conclusions

In this paper, an optimization-based steady-state model of the MMC was derived to calculate the converter's references considering its design limitations and the grid code constraints (regarding active and reactive power injection during AC grid voltage sag scenarios). To validate the algorithm, the optimization outputs are compared with the MMC's time-domain responses for different types of faults. For all the cases, the suggested method was able to meet the grid operator requirements while maintaining the converter's quantities within its limits.

References

- [1] D. Van Hertem, O. Gomis-Bellmunt, and J. Liang, *HVDC Grids: For Offshore and Supergrid of the Future*, ser. IEEE Press Series on Power Engineering. Wiley, 2016.
- [2] E. Prieto-Araujo, A. Junyent-Ferré, C. Collados-Rodríguez, G. Clariana-Colet, and O. Gomis-Bellmunt, "Control design of modular multilevel converters in normal and AC fault conditions for HVDC grids," *Electr. Pow. Syst. Res.*, vol. 152, pp. 424 – 437, 2017.
- [3] X. Shi, Z. Wang, B. Liu, Y. Li, L. M. Tolbert, and F. Wang, "Steady-state modeling of modular multilevel converter under unbalanced grid conditions," *IEEE Trans. Power Electron.*, vol. 32, no. 9, pp. 7306–7324, Sep. 2017.
- [4] G. Bergna-Diaz, J. A. Suul, E. Berne, J. Vannier, and M. Molinas, "Optimal shaping of the MMC circulating currents for preventing AC-side power oscillations from propagating into HVDC grids," *IEEE Trans. Emerg. Sel. Topics Power Electron.*, vol. 7, pp. 1015–1030, June 2019.

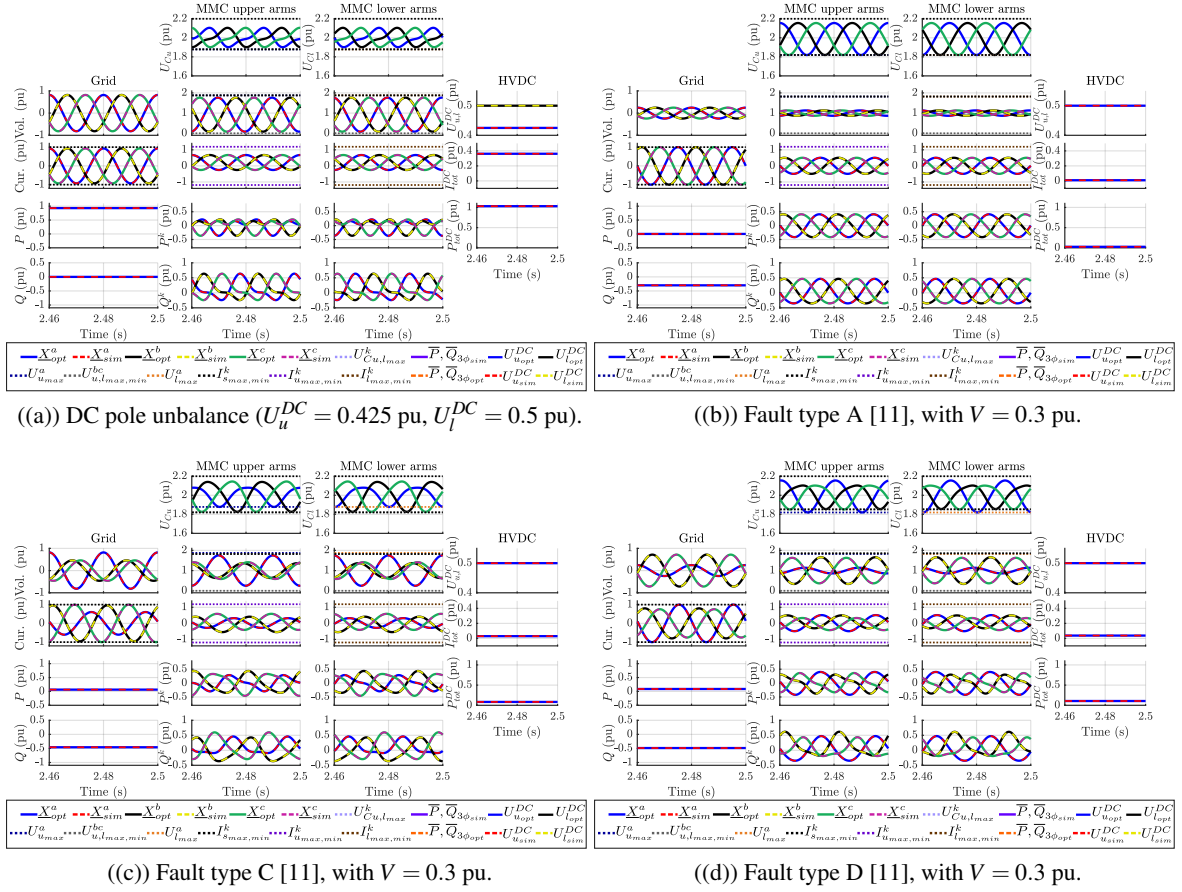


Fig. 3: Steady-state waveforms comparing the optimization outputs with the MMC response.

- [5] J. Li, G. Konstantinou, H. R. Wickramasinghe, and J. Pou, "Operation and control methods of modular multilevel converters in unbalanced AC grids: A review," *IEEE Trans. Emerg. Sel. Topics Power Electron.*, vol. 7, pp. 1258–1271, 2019.
- [6] D. W. Spier, J. L. Mestre, E. Prieto-Araujo, and O. Gomis-Bellmunt, "Steady-state analysis of the modular multilevel converter," in *IECON 2019 - 45th Annual Conference of the IEEE Industrial Electronics Society*, vol. 1, 2019, pp. 4861–4866.
- [7] K. Sharifabadi, L. Harnefors, H. Nee, S. Norrga, and R. Teodorescu, *Main-Circuit Design*, 2016, pp. 60–132.
- [8] D. W. Spier, E. Prieto-Araujo, J. Lopez-Mestre, and O. Gomis-Bellmunt, "Optimal current reference calculation for MMCs considering converter limitations," *IEEE Trans. Power Del.*, pp. 1–1, 2020.
- [9] National Grid TSO, *The Grid Code*, Nov. 2020. [Online]. Available: <https://www.nationalgrideso.com/document/162271/download>
- [10] B. O. del Estado, "Orden TED/749/2020, de 16 de julio, por la que se establecen los requisitos técnicos para la conexión a la red necesarios para la implementación de los códigos de red de conexión," no. 208, pp. 62 406–62 458, Aug. 2020.
- [11] M. Bollen and L. Zhang, "Different methods for classification of three-phase unbalanced voltage dips due to faults," *Electr. Power Syst. Res.*, vol. 66, no. 1, pp. 59 – 69, 2003.